Cellular/Molecular

Fibroblast Growth Factor Homologous Factor 2B: Association with $Na_v1.6$ and Selective Colocalization at Nodes of Ranvier of Dorsal Root Axons

Ellen K. Wittmack,[1,3,4] Anthony M. Rush,[2,3,4] Matthew J. Craner,[2,3,4] Mitchell Goldfarb,[5] Stephen G. Waxman,[2,3,4] and Sulayman D. Dib-Hajj[2,3,4]

Departments of [1]Pharmacology and [2]Neurology and [3]The Center for Neuroscience and Regeneration Research, Yale University School of Medicine, New Haven, Connecticut 06510, [4]Rehabilitation Research Center, Veterans Affairs Connecticut Healthcare System, West Haven, Connecticut 06516, and [5]Department of Biological Sciences, Hunter College of City University, New York, New York 10021

Voltage-gated sodium channels interact with cytosolic proteins that regulate channel trafficking and/or modulate the biophysical properties of the channels. $Na_v1.6$ is heavily expressed at the nodes of Ranvier along adult CNS and PNS axons and along unmyelinated fibers in the PNS. In an initial yeast two-hybrid screen using the C terminus of $Na_v1.6$ as a bait, we identified FHF2B, a member of the FGF homologous factor (FHF) subfamily, as an interacting partner of $Na_v1.6$. Members of the FHF subfamily share ~70% sequence identity, and individual members demonstrate a cell- and tissue-specific expression pattern. FHF2 is abundantly expressed in the hippocampus and DRG neurons and colocalizes with $Na_v1.6$ at mature nodes of Ranvier in myelinated sensory fibers in the dorsal root of the sciatic nerve. However, retinal ganglion cells and spinal ventral horn motor neurons show very low levels of FHF2 expression, and their axons exhibit no nodal FHF2 staining within the optic nerve and ventral root, respectively. Thus, FHF2 is selectively localized at nodes of dorsal root sensory but not ventral root motor axons. The coexpression of FHF2B and $Na_v1.6$ in the DRG-derived cell line ND7/23 significantly increases the peak current amplitude and causes a 4 mV depolarizing shift of voltage-dependent inactivation of the channel. The preferential expression of FHF2B in sensory neurons may provide a basis for physiological differences in sodium currents that have been reported at the nodes of Ranvier in sensory versus motor axons.

Key words: **dorsal root ganglia; sodium channels; nodes of Ranvier; yeast two-hybrid assay; ventral root; dorsal root**

Introduction

Voltage-gated sodium channels play an important role in electrogenesis in excitable cells (Catterall, 2000). To date, 10 different channels have been described and have been shown to differ in tissue and developmental expression patterns and pharmacology (Goldin et al., 2000). Sodium channels participate in the pathophysiology of epilepsy, cardiac arrhythmias, neuropathic pain, and multiple sclerosis; thus, they are considered important therapeutic targets.

$Na_v1.6$ (also termed SCN8A or PN4) is a sodium channel that is expressed throughout the CNS and the PNS (Burgess et al., 1995; Schaller et al., 1995) and is abundant at the axon initial segment, at the nodes of Ranvier (Caldwell et al., 2000; Krzemien et al., 2000; Tzoumaka et al., 2000; Boiko et al., 2001), and along nonmyelinated axons of the PNS (Black et al., 2002). $Na_v1.6$ produces a fast inactivating, TTX-sensitive (TTX-S) sodium current (Dietrich et al., 1998; Smith et al., 1998; Herzog et al., 2003b). Disruption in mice of *Scn8a*, the gene that encodes $Na_v1.6$, produces the motor endplate disease (*med*) resulting in juvenile lethality (Burgess et al., 1995), whereas several point mutations produce less severe neurological disorders (Meisler et al., 2002).

Several proteins have been found to bind to sodium channels and affect channel trafficking, anchoring at the cell surface, and biophysical properties. Sodium channel $\beta1$ and $\beta3$ subunits link the channel to extracellular matrix proteins via neurofascin-186 and may play a role in retaining sodium channels at the nodes of Ranvier (Ratcliffe et al., 2001). $Na_v1.6$ associates with ankyrin-G, βIV spectrin, and L1 cell adhesion molecules neurofascin and NrCAM at the initial segment (Jenkins and Bennett, 2001). Calmodulin binds to the IQ motif in the C termini of several sodium channels and produces isoform-specific changes in the properties of these channels (Mori et al., 2000; Deschenes et al., 2002; Tan et al., 2002; Herzog et al., 2003a). Calmodulin appears to regulate current density and slows the kinetics of inactivation of $Na_v1.6$ (Herzog et al., 2003a). Previously, we reported that a member of the FGF homologous factors (FHFs), FHF1B (Smallwood et al., 1996), binds to sodium channels $Na_v1.5$ and $Na_v1.9$ (Liu et al., 2001, 2003). FHF1B

Received April 28, 2004; revised June 14, 2004; accepted June 16, 2004.

This work was supported in part by grants from the National Multiple Sclerosis Society and the Rehabilitation Research Service and Medical Research Service, Department of Veterans Affairs. The Center for Neuroscience and Regeneration Research is a collaboration of the Paralyzed Veterans of America and the United Spinal Association with Yale University. E.K.W. was supported by a National Research Service Award predoctoral fellowship from the National Institute of Neurological Disorders and Stroke. We thank Dr. Joel Black for valuable discussions.

Correspondence should be addressed to Dr. Sulayman D. Dib-Hajj, The Center for Neuroscience and Regeneration Research, Veterans Affairs Connecticut Healthcare System, 950 Campbell Avenue, 127A, Building 34, West Haven, CT 06516. E-mail: sulayman.dib-hajj@yale.edu.

DOI:10.1523/JNEUROSCI.1628-04.2004

 0270-6474/04/246765-11$15.00/0

binding to $Na_v1.5$ causes a hyperpolarizing shift in steady-state inactivation (Liu et al., 2003).

To identify proteins that interact with $Na_v1.6$, we performed a genetic screen that identified FHF2 as a binding partner of $Na_v1.6$. We then investigated the interaction of FHF2 with $Na_v1.6$ *in vivo* and *in vitro*. We report in this study the association of FHF2 and sodium channels in native tissues and demonstrate the preferential colocalization of FHF2 and $Na_v1.6$ at nodes of Ranvier in sensory fibers of the dorsal root, but not in ventral root motor fibers or in optic nerve fibers. Additionally, we demonstrate that the coexpression of FHF2B and $Na_v1.6$ in the dorsal root ganglion (DRG)-derived cell line ND7/23 (Wood et al., 1990) increases the amplitude of the sodium current by ~2.5-fold and shifts the voltage dependence of inactivation in a positive direction.

Materials and Methods

Antibodies and mammalian cell lines. The anti-green fluorescent protein (GFP) antibody used in this study was purchased from Santa Cruz Biotechnology (Santa Cruz, CA). Monoclonal anti-sodium channel, pan antibody, and polyclonal anti-sodium channel PN4 were purchased from Sigma (St. Louis, MO) and Alomone (Jerusalem, Israel), respectively. The specificity of the anti-$Na_v1.6$ antibody is demonstrated by the lack of immunolabeling of neural tissues from *med* mice (Black et al., 2002), which are homozygotes for the *Scn8A* ^{med} null allele (Burgess et al., 1995). The anti-FHF2 antibody was designed against a peptide in the C terminus of the protein, and its characterization was published previously (Schoorlemmer and Goldfarb, 2002). The anti-Caspr antibody was a gift from Dr. M. Rasband (University of Connecticut Health Center, Farmington, CT). The mouse anti-IgG antibody used as a control for immunoprecipitation was purchased from Vector Laboratories (Burlingame, CA). The secondary anti-mouse IgG antibody for Western blot analysis was purchased from Dako (Carpinteria, CA). The secondary antibodies used for immunocytochemistry, goat anti-rabbit Alexa 488 (Cy2), goat anti-rabbit Alexa 568 (Cy3), and goat anti-mouse Alexa 633 (Cy5), were from Molecular Probes (Eugene, OR). Secondary antibodies 568 $F(ab')_2$ fragment of goat anti-rabbit IgG and Alexa Fluor 488 $F(ab')_2$ fragment of goat anti-rabbit IgG (Molecular Probes) were used in the colocalization experiments of FHF2 and $Na_v1.6$ in the hippocampus.

The DRG-derived cell line ND7/23 (Wood et al., 1990) was used to express $Na_v1.6$ channels. The ND7/23 cell line produces a TTX-S, but not a TTX-resistant (TTX-R), current (Zhou et al., 2003; John et al., 2004). The lack of a TTX-R current is consistent with the absence of TTX-R channel transcripts from these cells (data not shown). However, the ND7/23 cell line has been used successfully to express recombinant, TTX-R $Na_v1.8$ channels (Zhou et al., 2003; John et al., 2004). The human embryonic kidney 293 (HEK 293) cell line was used for coimmunoprecipitation experiments of FHF2B and $Na_v1.6$ because it produces very low levels of endogenous sodium channels.

Plasmids. For the initial yeast two-hybrid (Y2H) screen, a cDNA fragment encoding the C terminus of $Na_v1.6$ (aa1766–1976; GenBank accession number L39018) was cloned into the pGBKT7 plasmid (Clontech, Palo Alto, CA) at *Eco*RI/*Bam*HI sites (pGBKT7–1.6C). The pretransformed human embryonic cDNA library in pGADT7 (Matchmaker) was purchased from Clontech.

To confirm the binding of members of the FHF family to sodium channels, the yeast expression vector pDBleu (Invitrogen, Carlsbad, CA) was used to clone a *Sal*I-*Not*I fragment encoding the C terminus of $Na_v1.6$ in-frame with the Gal4 DNA-binding domain (pDBleu-Nav1.6C). The full coding sequence of human FHF1A (FGF12, transcript variant 2; GenBank accession number NM004113); rat FHF1B (GenBank accession number AF348446); human FHF2A (FGF13, isoform 1A; GenBank accession number BC034340); human FHF2B (FGF13, isoform 1B; GenBank accession number NM033642); human FHF2YV, FHF2Y, and FHF2V (FGF13, isoform 1Y1V; GenBank accession number AF108756); human FHF3 (FGF11; GenBank accession number NM004112); human FHF4A (FGF14; GenBank accession number NM004115); and rat FHF4B (FGF14B; GenBank accession number AB008908) were cloned in-frame into the yeast expression vector pPC86 (Invitrogen), allowing for the fusion of these factors to the VP16 transactivation domain. The plasmids generated were pPC86-FHF1A, pPC86-FHF1B, pPC86-FHF2A, pPC86-FHF2B, pPC86-FHF2Y, pPC86-FHF2V, pPC86-FHF2V+Y, pPC86-FHF4A, and pPC86-FHF4B. In addition, the conserved region of the FHF2 isoforms (nt 552–1104; GenBank accession number BC034340) was cloned into the *Not*I/*Sal*I sites of pPC86 to generate the plasmid pPC86-FHF2ΔN.

FHF2B cDNA was cloned into the plasmid pEGFP-N1 (Clontech) to produce a fusion protein in mammalian cells. This same FHF2B–GFP construct was used to test the association of $Na_v1.6$ and FHF2B in HEK 293 cells and to investigate the functional effect on the channel in ND7/23 cells. Primers were designed to amplify the full-length human FHF2B (FGF13, isoform 1B; GenBank accession number NM033642), and the PCR product was cloned in-frame into pEGFP-N1 at *Hind*III and *Bam*HI sites.

The mouse TTX-S $Na_v1.6$ channel was cloned into the mammalian expression vector pcDNA3.1, as reported previously (Herzog et al., 2003b). The $Na_v1.6$ channel was rendered TTX resistant ($Na_v1.6_R$) by changing tyrosine 371 in the pore region to serine, thus allowing the study of the $Na_v1.6$ current in cells in which endogenous TTX-S sodium channels are blocked by TTX in the bath (Herzog et al., 2003b).

The identity of all of the constructs were verified by sequencing of the inserts at the Howard Hughes Medical Institute/Keck Biotechnology Resource Laboratory at Yale University. Sequence analysis was done using the Basic Local Alignment Search Tool (BLAST; National Library of Medicine).

Y2H assay. The initial Y2H screen used the Matchmaker system according to the manufacturer's (Clontech) recommendations. Briefly, pGBKT7-$Na_v1.6C$ plasmid was used to transform the yeast strain AH109. This resultant strain was then mated with yeast strain Y187. Before mating, the Y187 strain was pretransformed with a human embryonic brain cDNA library that was fused to the Gal4 activation domain in pGADT7 (Clontech). Mating proceeded overnight, and the mated yeast were plated on quadruple dropout media SD/-Ade/-His/-Leu/-Trp to select for colonies containing both plasmids. Filter-lift β-galactosidase (β-gal) assay was done to identify positive interacting partners (Hollenberg et al., 1995).

The screen to identify the isoforms of the FHF family that bind voltage-gated sodium channels including $Na_v1.6$ was performed as described previously (Liu et al., 2003). We used the ProQuest system (Invitrogen) for these assays because it is easier to manipulate than the Matchmaker system. Briefly, bait plasmid pDBleu-$Na_v1.6C$ and the FHF constructs in pPC86 yeast vector were introduced into the yeast MaV203 strain, and transformants were selected on defined medium lacking leucine and tryptophan. After incubation at 30°C for 7 d, the colonies were screened for β-gal by a filter-lift assay (Hollenberg et al., 1995).

In vivo *coimmunoprecipitation.* One-sixth of the cerebral hemisphere of the brain of an adult male Sprague Dawley rat was extracted and homogenized in immunoprecipitation (IP) buffer of 20 mM Tris-HCl and 150 mM NaCl supplemented with protease inhibitors. Soluble proteins were extracted with 1% TritonX-100 for 15 min at 4°C and were collected in the supernatants after centrifugation at 20,000 × *g* for 20 min at 4°C. Protein A-Sepharose beads (Amersham Biosciences, Piscataway, NJ) were pre-blocked for 1 hr at 4°C in IP buffer supplemented with 3% BSA. The supernatant from the homogenized brain was pre-cleared with the blocked protein A-Sepharose at 4°C for 30 min. The beads were pelleted and discarded, and 2 μg of each antibody was added to an equal volume of the pre-cleared brain lysate. The antibody–brain mixture was incubated at 4°C for 2 hr before the addition of 50 μl of pre-blocked protein A agarose. The complex was incubated on a rotating platform at 4°C for 2 hr. The resin complex was washed three times in 0.1% TritonX-100 in PBS and three times in PBS and then denatured in 2× sample buffer at 37°C for 20 min. The proteins were separated by a 4–15% SDS-PAGE and transferred to immunoblot polyvinylidene difluoride (PVDF) membrane overnight at 20 V. The membrane was blocked in 10% dry milk for 1 hr and incubated in primary pan sodium channel antibody (1 μg/ml) for 2 hr. The membrane was then washed for 30 min and incubated with secondary antibody (anti-mouse IgG; 0.1 μg/ml) for

1 hr at room temperature. The membrane was washed, and the signal was detected using the ECL Plus chemiluminescent system.

Coimmunoprecipitation from transfected HEK 293 cells. Because we did not achieve reproducible Western blot and IP results with the anti-$Na_v1.6$ antibody, we investigated the coimmunoprecipitation of FHF2B and $Na_v1.6$ in transiently transfected HEK 293 cells. HEK 293 cells were cultured on 10 cm dishes and were transfected at 80% confluency using the LipofectAMINE 2000 reagent according to the manufacturer's (Invitrogen) recommendation. Briefly, 8 μg of pEGFP-N1 or FHF2-GFP and 16 μg of pCDNA3-$Na_v1.6_R$ were added to 1.5 ml of DMEM without serum and antibiotics. LipofectAMINE 2000 (60 μl) was added to a separate tube containing 1.5 ml of DMEM (without serum and antibiotics). The two solutions were mixed together gently and incubated at room temperature for 20 min before being added to the HEK 293 cells. The cells were incubated at 37°C for 24 hr.

For the coimmunoprecipitation experiment, each 10 cm dish of transfected HEK 293 cells were suspended in 500 μl of IP buffer, and IP of the protein complex by anti-GFP antibody (Santa Cruz Biotechnology) and Western blot assay using pan sodium channel antibody were performed as described above. Western blotting of cell lysates with the anti-GFP and pan sodium channel antibodies was used to show expression of GFP, FHF2B-GFP, and $Nav1.6_R$ in the transfected cells.

Immunohistochemistry. Adult Sprague Dawley rats were anesthetized with ketamine (80 mg/kg, i.p.) and xylazine (50 mg/kg) and perfused with 4% paraformaldehyde in 0.01 M PBS. Tissues were postfixed in 4% paraformaldehyde for 30 min, rinsed in PBS, and cryoprotected overnight in 30% sucrose in PBS. The DRG and hippocampus were cryosectioned into 12 and 10 μm slices, respectively, whereas dorsal root, ventral root, and optic nerve were cryosectioned into 6 μm slices. The slides were desiccated overnight and processed for immunohistochemistry. Because both antibodies against $Na_v1.6$ and FHF2 are rabbit polyclonal antibodies, it was necessary to incubate the sections sequentially. For processing of the DRG, dorsal root, ventral root, and optic nerve, sections were incubated in blocking solution (PBS with 5% normal horse serum and 1% BSA) with 0.1% Triton X-100 and 0.02% sodium azide at room temperature for 30 min. The slides were incubated with anti-$Na_v1.6$ antibody (1:100; Alomone) overnight at 4°C. The next day, the slides were washed six times for 5 min each and then incubated with goat anti-rabbit Alexa 568 Cy3 (1:1000; Molecular Probes) for 3 hr at room temperature. After six washes, the slides were incubated with anti-FHF2 antibody (1:100) and anti-Caspr antibody (1:500; a gift from M. Rasband) for 3 hr, washed as described above, and then incubated in goat anti-rabbit Alexa 488 Cy2 (1:1000; Molecular Probes) and goat anti-mouse Alexa 633 Cy5 (1:1000; Molecular Probes) for 3 hr. Colocalization in DRG neurons was done as described above, but without the Caspr antibody. As a control to insure that Cy2 labeling is specific to FHF2 and not attributable to a cross reaction with the $Na_v1.6$ antibody, slides were processed as described above with the omission of anti-FHF2 or goat anti-rabbit Alexa 488 Cy2 and showed no staining. In addition, the dorsal and ventral roots of four animals were processed by nonsequential immunohistochemistry with the anti-FHF2 and anti-Caspr antibodies to confirm the results from the sequential experiment and to quantitate the number of positive dorsal and ventral nodes among the four animals. Images show that FHF2 antibodies immunolabel nodes in the dorsal root (supplemental Fig. 1, available at www.jneurosci.org/cgi/content/full/24/30/6765/DC1), thus providing additional evidence that FHF2 immunostaining in the triple labeling experiments with $Na_v1.6$, FHF2 and Caspr is not an artifact of the sequential addition of the antibodies (see above).

The hippocampus was processed serially with the $Na_v1.6$ and FHF2 antibodies as described above with the following modification. After the overnight incubation with the anti-$Na_v1.6$ antibody, the slides were washed and then incubated with Alexa Fluor 568 $F(ab')_2$ fragment of goat anti-rabbit IgG (1:1000; Molecular Probes) for 3 hr at room temperature. After six washes, the slides were incubated with anti-FHF2 antibody overnight at 4°C. The next day, the slides were washed and incubated with Alexa Fluor 488 $F(ab')_2$ fragment of goat anti-rabbit IgG (1:1000; Molecular Probes) for 3 hr at room temperature, washed, covered with 25% glycerol, and viewed. The $F(ab')_2$ fragments were used in this experiment to minimize possible interactions of the FHF2 antibody with the Fc unoccupied binding site of the Alexa Fluor 568 goat anti-rabbit IgG.

To examine the localization of FHF2 in unmyelinated axons, sciatic nerves of adult rat were teased using the following protocol. Sciatic nerves were dissected from adult Sprague Dawley rats and were incubated immediately in 4% paraformaldehyde for 10 min. The nerves were transferred to 30% sucrose in PBS for cryoprotection. The sciatic nerves were incubated in Complete saline solution supplemented with 10 mg of collagenase D and 10 mg of collagenase A at 37°C for 20 min before washing three times with PBS. Nerves were teased on the slides and desiccated overnight. The following day, the slides were blocked for 30 min, as described above, and then incubated overnight with anti-FHF2 and anti-peripherin (1:100; NovoCastra, Newcastle, UK) antibodies. The next day, the slides were washed six times with PBS and then incubated with goat anti-rabbit Alexa 568 Cy3 and goat anti-mouse Alexa 488 Cy2 for 3 hr at room temperature.

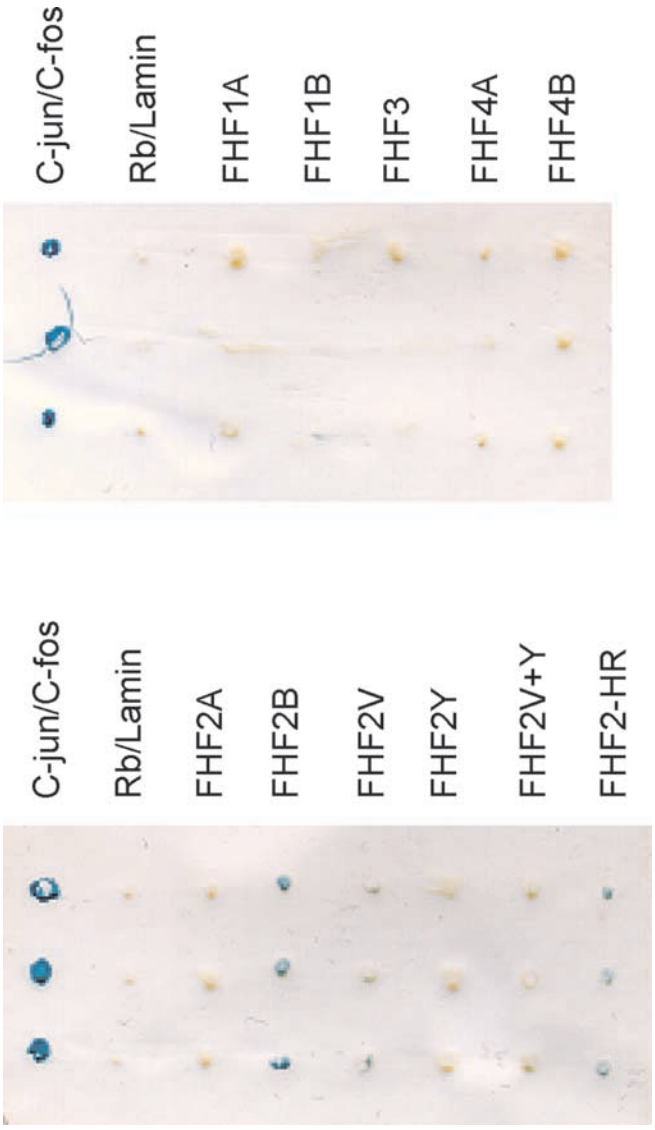

Figure 1. $Na_v1.6$ binds to several FHF2 isoforms in a Y2H assay. FHF members were expressed as fusion proteins with the VP16 activation domain, and the C terminus of $Na_v1.6$ was expressed as a fusion protein with the Gal4 DNA-binding domain. Pairwise binding of $Na_v1.6C$ and members of the FHF family, as indicated, was tested by the filter-lift β-gal assay. A blue signal indicates a positive interaction between the two proteins. The interacting partners c-*jun*/c-*fos* served as a positive controls, and the noninteracting pair Rb/lamin served as a negative control.

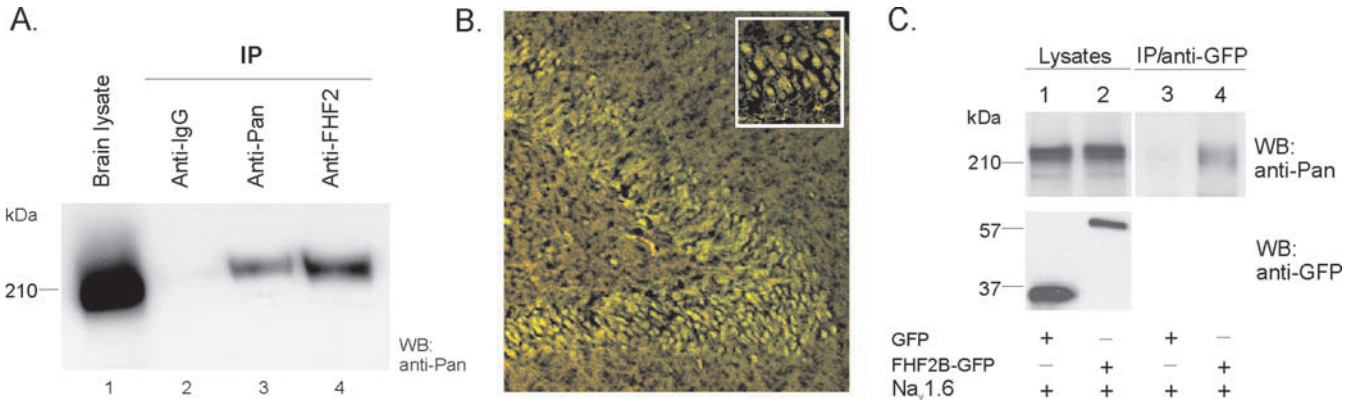

Figure 2. FHF2 and Na$_v$1.6 are colocalized in the brain. *A*, Pan sodium channel and FHF2 antibodies were used to immunoprecipitate (IP) the voltage-gated sodium channels from a rat brain lysate. Anti-mouse IgG was used as a negative control to rule out nonspecific binding. Western blotting analysis of the IP complex was performed by the pan sodium channel antibody. Lane 1 shows a robust immunoreactive signal from the cell lysate that was used for the IP assay, consistent with the presence of intact sodium channel proteins in this sample. Nonspecific antibodies do not immunoprecipitate a channel complex (lane 2). As predicted, pan sodium channel antibody immunoprecipitated a channel complex (lane 3). The reduced signal in lane 3 compared with lane 1 is likely attributable to the avidity of the antibody in the two different assays. FHF2 coimmunoprecipitated voltage-gated sodium channels from the brain lysate (lane 4). Comparison of the immunoreactive bands in lanes 1 and 4 might be explained by the interaction of FHF2 with only a subset of the cellular pool of channels. The molecular weight marker (in kilodaltons) is shown on the left. *B*, Colocalization of Na$_v$1.6 and FHF2 in the hippocampus. Na$_v$1.6- and FHF2-specific antibodies were used to immunolabel sections of rat hippocampus. FHF2 (green) and Na$_v$1.6 (red) proteins were detected in the pyramidal cells of Ammon's horn, and the merged images (yellow) show significant colocalization of the two proteins. The inset shows the pyramidal cells at 40× magnification. *C*, GFP antibody was used to IP Na$_v$1.6 from lysates of HEK 293 cells transfected with either Na$_v$1.6 plus GFP (control; lane 3) or Na$_v$1.6 plus FHF2B-GFP (lane 4). The IP complex was probed with the pan sodium channel antibody and detected no association between Na$_v$1.6 with GFP (lane 3), but an association of Na$_v$1.6 with FHF2B (lane 4). Lanes 1 and 2 show Western blotting analysis of the cell lysates probed with pan sodium channel antibody (top) and GFP (bottom) to show comparable levels of Na$_v$1.6/GFP (lane 1) and Na$_v$1.6/FHF2B-GFP (lane 2) in the samples used for the immunoprecipitation assay.

After secondary antibody incubations, the slides were washed with PBS, covered with 25% glycerol, and viewed under a Nikon Eclipse E800 microscope fitted with a Nikon PCM-2000 laser for scanning confocal microscopy. Images were captured with SimplePCI and processed with Adobe Photoshop version 5.5.

In situ *hybridization.* A region of 368 nucleotide residues in the 3′ untranslated region (UTR) of FHF2B (nt 664–1031; GenBank accession number NM033642) was used to design the riboprobe. A BLAST search of the GenBank database using this sequence as query did not return matches other than FHF2 sequences. This segment was amplified from a human brain cDNA template and cloned in the vector pPCR-Script (Stratagene, La Jolla, CA). T7 and T3 RNA transcription was done separately using MEGAscript (Ambion, Austin, TX) and digoxigenin-labeled UTP on linearized plasmids to produce sense and antisense riborobes.

Rats were anesthetized and perfused as described above. Tissue was postfixed and cryoprotected overnight at 4°C in 4% paraformaldehyde with 30% sucrose. Serial 12 μm sections of DRG, cerebellum, retina, and lumbar enlargement of the spinal cord were cut onto slides and desiccated overnight. Sections were processed for *in situ* hybridization as described previously (Black et al., 1996), except that incubation in 4% paraformaldehyde was increased to 12 min and incubation in proteinase K was reduced to 6 min. Detection was done using a chromagen solution of 4-nitroblue tetrazolium chloride and 5-bromo-4-chloro-3-indolyl phosphate. Sense riboprobes yielded no signals in the *in situ* hybridization experiments.

Electrophysiology. Transfection of the ND7/23 cells was done as described above for the HEK 293 cells, but with the following modifications. The cells were plated at low density on 35 mm dishes 24 hr before transfection. Cells were transfected with 2 μg of either Na$_v$1.6 and GFP or Na$_v$1.6 and FHF2-GFP, and electrophysiology was performed 24 hr after transfection. Data presented here were collected from three independent transfections.

Whole-cell voltage-clamp recordings of transfected ND7/23 cells were made using an Axopatch 200B amplifier (Axon Instruments, Foster City, CA). Only cells with a robust GFP fluorescence signal (GFP or FHF2B-GFP) were used for recording. The pipette solution contained (in mM) 140 CsF, 1 EGTA, 10 NaCl, and 10 HEPES, pH 7.3, adjusted to 310 mOsm/l with glucose. The external solution contained (in mM) 140 NaCl, 3 KCl, 1 $MgCl_2$, 1 $CaCl_2$, 20 TEACl, 5 CsCl, 0.1 $CdCl_2$, 10 HEPES, and 0.00025 TTX, pH 7.3, adjusted to 320 mOsm/l with glucose. The pipette potential was adjusted to zero before seal formation, and the voltages were not corrected for liquid junction potential. Capacity transients were cancelled, and series resistance was compensated by 85–90%. Leakage current was subtracted digitally online using hyperpolarizing potentials applied after the test pulse (P/6 procedure). Currents were acquired using Clampex 8.1 software, filtered at 5 kHz and at a sampling rate of 20 kHz via a Digidata 1200 series interface (Axon Instruments). For current density measurements, the currents were divided by the cell capacitance, as read from the amplifier. All experiments were performed at room temperature (21–25°C). Data are expressed as mean ± SEM, and statistical analyses were performed using the Student's *t* test (significance at least $p < 0.05$).

Voltage protocols were implemented at predetermined times from going whole cell. Briefly, standard current–voltage (*I–V*) families were obtained using 40 msec pulses from a holding potential of −120 mV to a range of potentials (−65 to +60 mV) every 5 sec. The peak value at each potential was plotted to form *I–V* curves. Activation curves were fitted with the following Boltzmann distribution equation: $G_{Na} = G_{Na,max}/[1 + \exp(V_{1/2} - V_m)/k]$, where G_{Na} is the voltage-dependent sodium conductance, $G_{Na,max}$ is the maximal sodium conductance, $V_{1/2}$ is the potential at which activation is half-maximal, V_m is the membrane potential, and k is the slope. Availability protocols consisted of a series of pre-pulses (−120 to +20 mV) lasting 500 msec from the holding potential of −120 mV, followed by a 40 msec depolarization to −10 mV every 10 sec. The normalized curves were fitted using a Boltzmann distribution equation: $I_{Na}/I_{Na,max} = 1/[1 + \exp((V_m - V_{1/2})/k)]$, where $I_{Na,max}$ is the peak sodium current elicited after the most hyperpolarized prepulse, V_m is the preconditioning pulse potential, $V_{1/2}$ is the half-maximal sodium current, and k is the slope factor. Development of closed state inactivation at −70 mV was measured by holding cells at −120 mV, prepulsing to −70 mV for increasing amounts of time (1–3000 msec), and then stepping to −10 mV to determine the fraction of current inactivated during the pre-pulse. For recovery from inactivation experiments, two 40 msec stimuli were given to −10 mV from the holding potential of −120 mV, with a variable recovery time period at −80 mV, in the range of 0.1 to 200 msec. Curves were fitted with a double rising exponential function.

Because the Na$_v$1.6$_R$ channel is resistant to TTX (Herzog et al., 2003b), all recordings were done with 250 nM TTX in the bath. Endogenous TTX-S currents in ND7/23 are completely blocked under these condi-

tions. Thus, the amplitude and properties of $Na_v1.6$ could be investigated when expressed together with GFP or FHF2B-GFP in ND7/23 cells.

Results

Identification of members of the FHF family as binding partners of $Na_v1.6$

We performed an initial Y2H screen of a human embryonic brain cDNA library to identify proteins that interact with the $Na_v1.6$ C terminus, using the Matchmaker Y2H system. We screened two million clones and identified 11 clones that activated three reporter genes and remained positive after retransforming the yeast with the purified target plasmids and bait. Two members of the FHF family, partial segments of FHF2 and FHF4, were among the identified targets.

To determine the specific isoforms of the FHF family that may bind to the C terminus of $Na_v1.6$, we used Y2H/β-gal filter-lift assay (Fig. 1). The full-length clones of isoforms FHF1A, FHF1B, FHF2A, FHF2B, FHF2V, FHF2Y, FHF2V+Y, FHF3, FHF4A, and FHF4B were cloned into the pPC86 vector and screened for their ability to interact with the C terminus of $Na_v1.6$ (cloned into the pDBleu vector). In addition, the region of FHF2 that is encoded by exons 2–5 and that is conserved among all FHF2 isoforms (aa 10–192 of FHF2B) was cloned into pPC86 (FHF2ΔN). FHF2B, FHF2V, and FHF2 ΔN isoforms were found to bind to the C terminus of $Na_v1.6$ (Fig. 1). Interestingly, the full-length isoforms of FHF4 (FHF4A and FHF4B) did not bind to $Na_v1.6$C in this ProQuest-based assay, whereas a partial FHF4 was able to bind the $Na_v1.6$C when assayed in the Matchmaker system (see above).

In vivo evidence for the binding of FHF2 with voltage-gated sodium channels

We next sought to determine whether the interaction of $Na_v1.6$ and FHF2B in the Y2H assay reflects the interaction of the two proteins *in vivo*. Rat brain was homogenized in lysis buffer, and coimmunoprecipitation experiments were undertaken using FHF2-specific antibody to pull down sodium channels. A lysate sample (1/10 the volume used for IP) was saved and run on the gel as a positive control to verify the presence of intact channels in the sample. The lysate–antibody mixture was incubated with protein A-Sepharose for 2 hr and washed extensively before running on a SDS-PAGE 4–15% gradient gel. The gel was transferred to PVDF and probed with a monoclonal pan sodium channel antibody that binds to the highly conserved linker between domains III and IV of sodium channels. Figure 2*A* shows the results of the coimmunoprecipitation experiment from rat brain. Lane 1 contains the brain lysate and serves as a positive control for the Western blot. Lane 2 contains the IP complex using nonspecific mouse anti-IgG antibody, which serves as a negative control. As expected, the negative control does not show a protein band that reacts with the pan sodium channel antibody. Lane 3 shows, as expected, a sodium channel-immunoreactive band that was pulled down by the pan sodium channel antibody. Finally, lane 4 shows a sodium channel-immunoreactive band that was pulled down by the FHF2 antibody. The coimmunoprecipitation of sodium channels and FHF2 provides strong evidence that the two proteins are part of the same complex in brain tissue.

To confirm the colocalization of FHF2 and $Na_v1.6$ in the same cells in the brain tissue, we analyzed immunolabeling of hippocampus sections in which FHF2 expression was previously reported (Smallwood et al., 1996; Munoz-Sanjuan et al., 2000). Figure 2*B* shows the merged images (yellow) of $Na_v1.6$ (red) and FHF2 (green) in Ammon's horn of the hippocampus. Pyramidal cells are shown at higher magnification (40×) in the inset. The yellow color indicates substantial colocalization of the two proteins in these cells.

In vitro evidence for the binding of FHF2 to $Na_v1.6$

The commercial anti-$Na_v1.6$ antibody did not generate reproducible Western blot and IP results. Therefore, to verify that $Na_v1.6$ forms a complex with FHF2B, we performed immunoprecipitation experiments from HEK 293 cells transiently transfected with the two constructs (Fig. 2*C*). The two plasmids, pCDNA-$Na_v1.6_R$ and FHF2B-GFP, were cotransfected into HEK 293 cells. As a negative control, $Na_v1.6$ was also transfected into HEK 293 cells with GFP construct. Twenty-four hours after transfection, cells were collected, washed with PBS, and lysed in IP buffer. After brief centrifugation to remove cell debris, the supernatants were incubated with the anti-GFP antibody for 2 hr and protein A-Sepharose for 2 hr, both at 4°C. The beads were washed, boiled in 2× SDS-PAGE sample buffer, and run on a 4–15% gradient gel. Cell lysates were incubated at 37°C for 30 min before loading on the gel. Western blot analysis was done using the pan sodium channel antibody to detect $Na_v1.6$ in the IP complex.

Figure 2*C* shows the results of coimmunoprecipitation experiments using transfected HEK 293 cells. Western blotting was done with the anti-GFP antibody and pan sodium channel antibody to assess levels of GFP and FHF2B-GFP and $Na_v1.6$ in the IP reaction. Lanes 1 and 2 show the cell lysates for the HEK 293 cells transfected with $Na_v1.6$ and GFP (lane 1) and $Na_v1.6$ and FHF2B-GFP (lane 2) blotted with the pan antibody (top) and GFP antibody (bottom) to show expression levels of the recombinant proteins in the cell lysates. Comparison of the immunoreactive bands in lanes 1 and 2 shows that comparable levels of the recombinant proteins are present in the lysates, which were used for the coimmunoprecipitation experiments. Lanes 3 and 4 show the results of the pan sodium channel-antibody probing on the Western blot

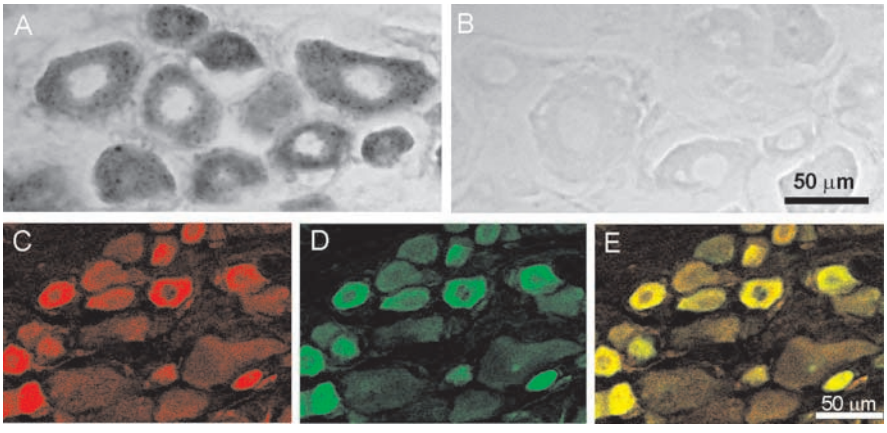

Figure 3. FHF2 is expressed in neurons of dorsal root ganglion. *In situ* hybridization using digoxigenin-labeled antisense (*A*) and sense (*B*) probes is shown. Significant staining of DRG neurons of all size classes was observed using the antisense probe (*A*). Sense riboprobes yielded no signals (*B*). Immunohistochemistry was performed using $Na_v1.6$- and FHF2-specific antibodies. Slides were viewed under a Nikon Eclipse E800 microscope. FHF2 (*C*) and $Na_v1.6$ (*D*) proteins were detected in small and large DRG neurons. A merge of the two images (*E*) shows significant colocalization of the two proteins. Scale bars, 50 μm.

assay of the IP complex. It is clear that the GFP antibody pulled down $Na_v1.6$ when it was cotransfected with FHF2B-GFP (lane 4), but not in the control transfection of GFP and $Na_v1.6$ (lane 3). This evidence strongly suggests that $Na_v1.6$ can exist in a protein complex with FHF2B.

FHF2 protein and mRNA in dorsal root ganglion neurons

The colocalization of FHF2 and $Na_v1.6$ in hippocampus neurons suggested that colocalization of the FHF2 protein with $Na_v1.6$ might also occur in neurons of the DRGs, where both $Na_v1.6$ and FHF2 are known to be expressed (Black et al., 1996; Li et al., 2002). To ascertain the expression of FHF2 mRNA within different subpopulations of DRG neurons, we produced a digoxigenin-labeled riboprobe that is predicted to hybridize to a 368 nucleotide sequence in the 3′ UTR of FHF2. Results of *in situ* hybridization experiments using the antisense and sense probes are shown in Figure 3, *A* and *B*. Whereas sense riboprobes produced only background staining (Fig. 3*B*), FHF2 transcripts were detected in small (<25 μm in diameter), medium (25–40 μm), and large (>40 μm) DRG neurons (Fig. 3*A*).

The expression and colocalization of FHF2 and $Na_v1.6$ in DRG neurons at the protein level was determined by immunocytochemistry, using FHF2- and $Na_v1.6$-specific antibodies. Immunohistochemistry was done on 12 μm slices of the L4/L5 DRG from adult rats, and the antibodies were added sequentially, as described in Materials and Methods. Figure 3 shows $Na_v1.6$ protein (Fig. 3*C*), FHF2 protein (Fig. 3*D*), and illustrates the colocalization of the proteins in neurons of all sizes (Fig. 3*E*). To confirm the distribution of FHF2 in DRG neurons, sections were incubated with the FHF2 antibody alone, and the expression of FHF2 in all classes of DRG neurons was confirmed (data not shown). As a marker for small-diameter DRG neurons, we used $Na_v1.9$, which is known to be selectively expressed in small DRG neurons (Dib-Hajj et al., 1998; Fang et al., 2002), and obtained significant colocalization with FHF2 (data not shown).

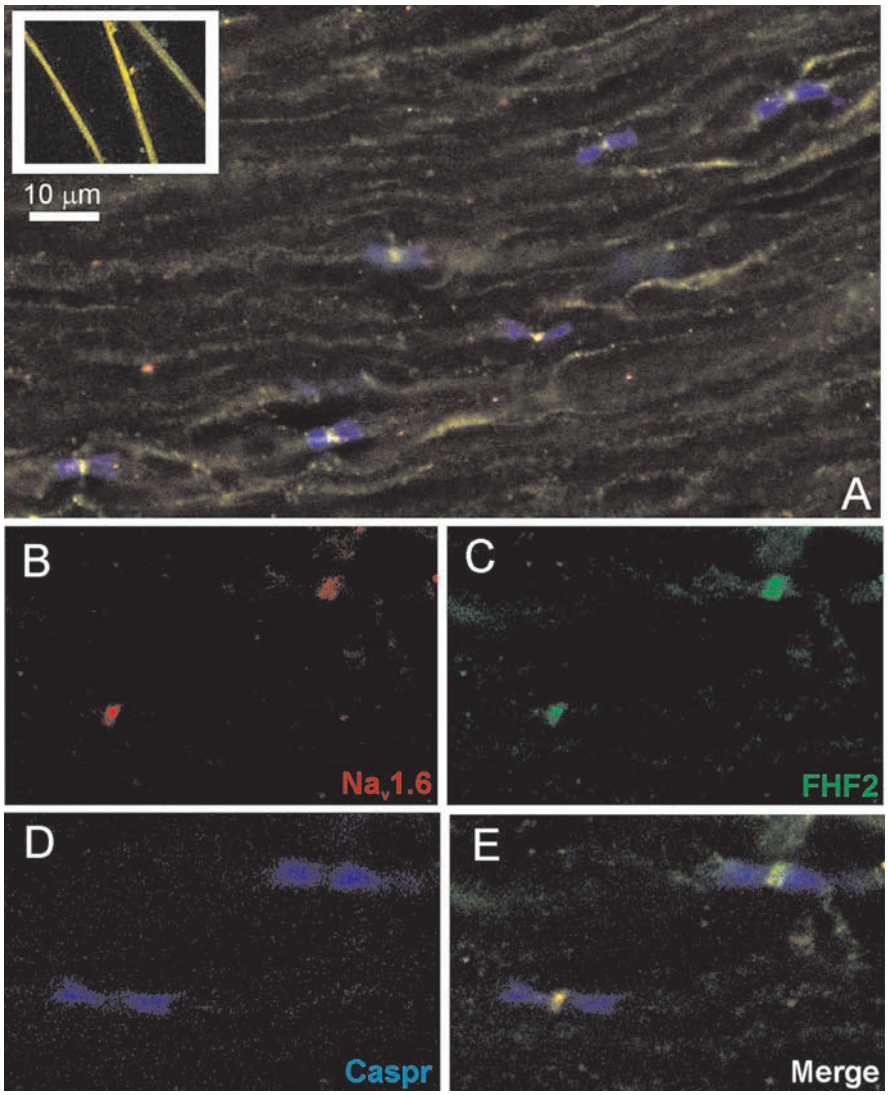

Figure 4. FHF2 is expressed at the nodes of Ranvier in the dorsal roots, where it colocalizes with $Na_v1.6$. Images of a section of the dorsal root immunolabeled with antibodies against $Na_v1.6$ (red), FHF2 (green), and Caspr (blue) show the colocalization of FHF2 and $Na_v1.6$, with $Na_v1.6$ present at every node of Ranvier, which shows FHF2 expression (*A*). Nodal regions were delineated by staining for Caspr, which is a marker of paranodes (*D*). As expected, $Na_v1.6$ staining was limited to the narrow gaps representing the nodes (*B*). FHF2 staining is restricted to a narrow band (*C*). The colocalization of $Na_v1.6$ and FHF2 at the nodes of Ranvier is demonstrated by the merger of the three images (*E*). Scale bar, 10 μm. The inset in *A* shows FHF2 in unmyelinated axons of the teased sciatic nerve. The picture is a merged image (yellow) of FHF2 (green) and peripherin (red), a marker of unmyelinated axons.

Nodal expression of FHF2

We have previously shown that $Na_v1.6$ is expressed in small-diameter DRG neurons and along their unmyelinated axons (Black et al., 2002). $Na_v1.6$ and FHF2 colocalized in small DRG neurons (Fig. 3). Therefore, we investigated the distribution of FHF2 in unmyelinated axons of the sciatic nerve. Teased sciatic nerve fibers were immunolabeled with peripherin, which is a marker of unmyelinated axons, and the FHF2-specific antibody. Consistent with the expression of FHF2 in small-diameter DRG neurons (Li et al., 2002) (Fig. 3), FHF2 is present in unmyelinated axons that arise from these neurons (Fig. 4*A*, inset).

Because $Na_v1.6$ is the major nodal sodium channel isoform (Caldwell et al., 2000; Krzemien et al., 2000; Tzoumaka et al., 2000; Boiko et al., 2001), we investigated the colocalization of FHF2 and $Na_v1.6$ at the nodes of Ranvier. Myelinated A-type fibers, which arise from large-diameter DRG neurons, project to the spinal cord via the dorsal root and to peripheral targets via the sciatic nerve. Nodes of Ranvier were delimited by labeling of tissue sections with Caspr, a marker of the paranodal region of the nodes of Ranvier (Peles and Salzer, 2000). Initial experiments using FHF2-specific antibody revealed a large number of FHF2-positive nodes in the roots entering the DRG, but there were also FHF2-negative nodes in the sciatic nerve (data not shown). To determine whether nodes of sensory and motor fibers differ in their composition, we investigated nodes of Ranvier in the dorsal and ventral roots of the spinal cord for the colocalization of FHF2 and $Na_v1.6$ (Fig. 4). Triple labeling with anti-Caspr, anti-FHF2, and anti-$Na_v1.6$ demonstrates colocalization of

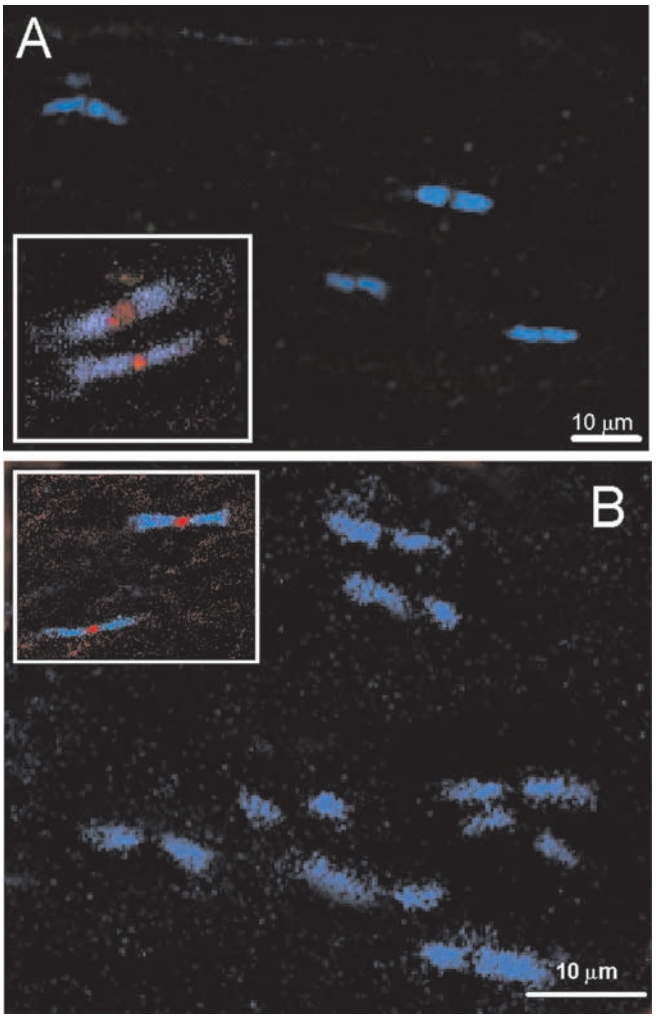

Figure 5. FHF2 is not expressed at the nodes of Ranvier in ventral roots or optic nerve. Images of a section of the ventral root (*A*) and optic nerve (*B*) immunolabeled with antibodies against $Na_v1.6$ (red), FHF2 (green), and Caspr (blue) are shown. Nodal regions were delineated by Caspr staining. As expected, $Na_v1.6$ staining was limited to the narrow gaps at nodes (*A*, *B*, insets). No FHF2 staining is detectable in either tissue. The staining of the nodes by $Na_v1.6$ argues against the possibility that the FHF2 antibody could not access the nodal region. Scale bar, 10 μm.

$Na_v1.6$ and FHF2 at nodes of the dorsal sensory root (Fig. 4). Similar experiments investigating the ventral motor root failed to show FHF2 at the nodes of Ranvier (Fig. 5*A*). Staining with anti-$Na_v1.6$ and anti-Caspr was positive in both cases, indicating that efficient antibody penetration at nodes in the motor root had occurred (Fig. 5, insets). Additionally, the lack of FHF2 labeling and $Na_v1.6$ labeling at nodes of the motor root is further indication that sequential addition of the antibodies did not result in artifactual labeling by the FHF2 antibody, and a similar pattern of differential FHF2 nodal labeling was obtained when only FHF2 and Caspr antibodies were used for the coimmunostaining (supplemental Fig. 1, available at www.jneurosci.org/cgi/content/full/24/30/6765/DC1). We also investigated the presence of FHF2 at nodes of Ranvier in the optic nerve with antibodies against FHF2, $Na_v1.6$, and Caspr. Figure 5*B* shows that these nodes do not contain detectable levels of FHF2.

To quantitiate the preferential expression of FHF2 at the nodes in the dorsal sensory root but not in the ventral motor root, we counted 100 nodes in both the sensory and motor roots in each of four animals. Immunostaining experiments were performed using antibodies against FHF2 and Caspr. These experiments show that FHF2 is present at nodes of the dorsal sensory root but not at nodes in the ventral motor root (data not shown). Analysis of these images show that in the sensory roots, 98.5% of the nodes were positive for FHF2, whereas in the motor root, <1% of the nodes were positive. Analysis of the intensity of FHF2 staining in the sensory root showed no difference in intensity of FHF2 staining between small (<2 μm), medium (2–5 μm), and large (>5 μm) diameter nodes.

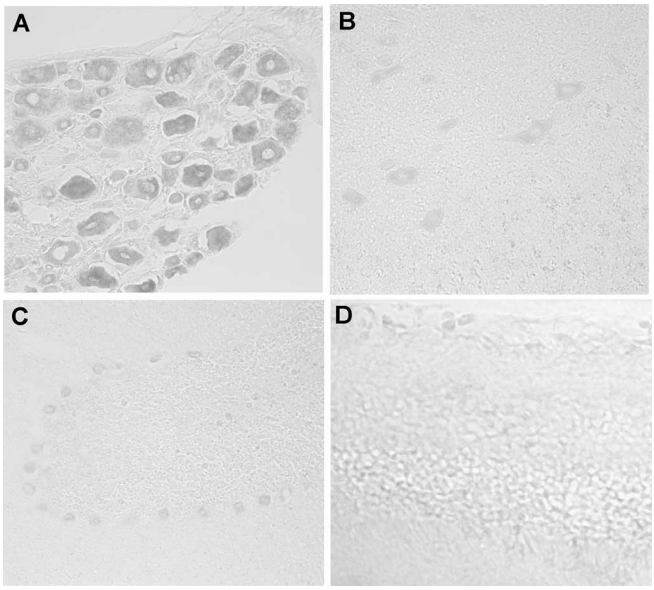

Figure 6. Expression of FHF2 mRNA in DRG neurons, ventral horn of spinal cord, Purkinje neurons, and retinal ganglion neurons. *In situ* hybridization using FHF2 digoxigenin-labeled riboprobe shows that FHF2 is abundantly expressed in DRG neurons (*A*) compared with motor neurons in the ventral horn (*B*), Purkinje cells (*C*), or retinal ganglion neurons (*D*). All tissues were processed together, and the colorimetric reaction was stopped before it reached saturation to allow a comparison of the levels of FHF2 expression.

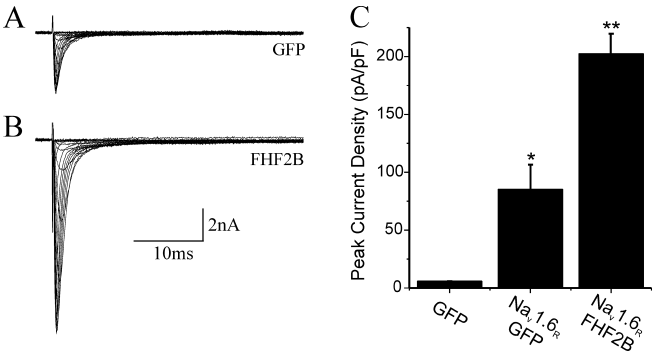

Figure 7. FHF2B increases functional Na_v 1.6 sodium current density in transiently transfected ND7/23 cells. Representative examples of sodium current traces are shown. ND7/23 cells were transiently transfected with Na_v 1.6_R and either GFP (*A*) or FHF2B-GFP (*B*). Cells were held at a potential of −120 mV and depolarized to a range of potentials (−65 to +60 mV) for 40 msec. *C*, Maximum peak current densities were measured and plotted (pA/pF). Cells transfected with GFP alone showed essentially zero sodium current (6.0 ± 0.5 pA/pF; $n = 11$) compared with those transfected with Na_v 1.6_R and GFP, which displayed robust transient sodium currents (85.4 ± 21.2 pA/pF; $n = 11$; $^*p < 0.005$). Cells transfected with Na_v 1.6_R and FHF2B-GFP (202.5 ± 17.5 pA/pF; $n = 22$) produced a more than twofold increase in current density when compared with cells transfected with Na_v 1.6 and GFP control (85.4 ± 21.2 pA/pF; $n = 11$; $^{**}p < 0.001$).

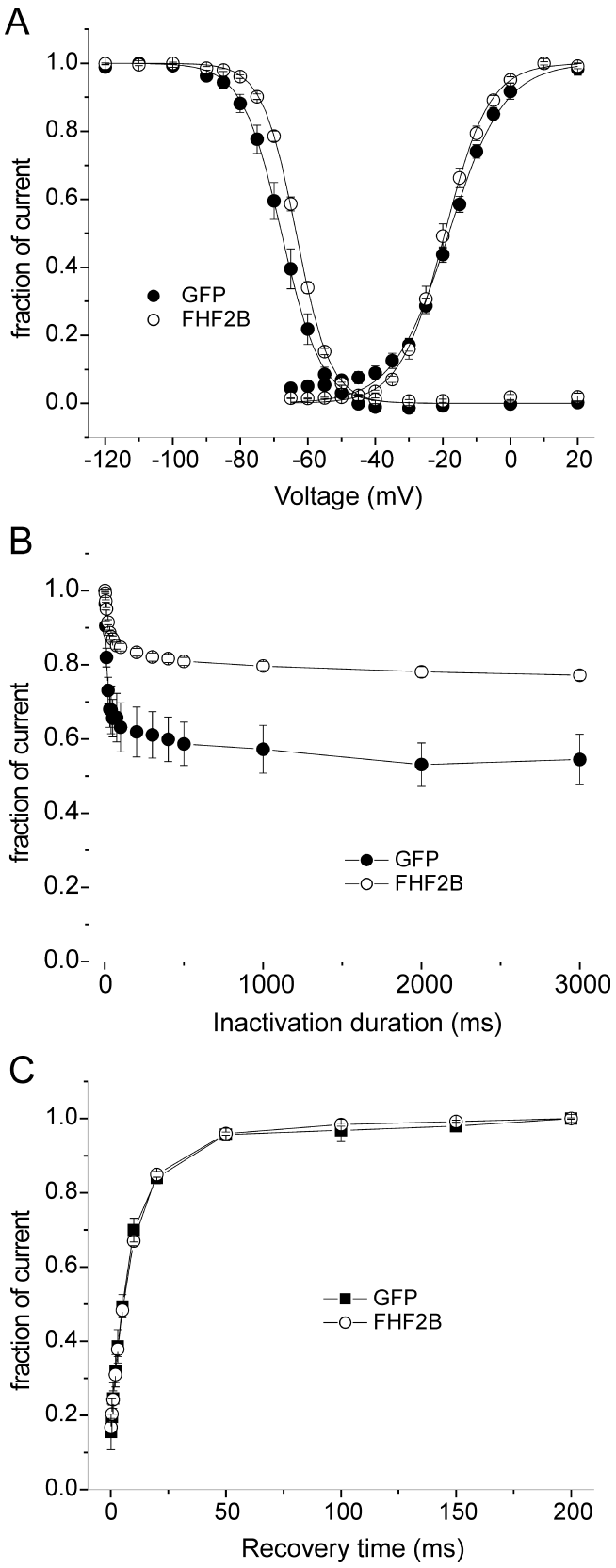

Figure 8. FHF2B causes a depolarizing shift in steady-state inactivation of Na_v 1.6 sodium currents. *A*, Steady-state activation and inactivation curves are shown for ND7/23 cells transiently transfected with Na_v 1.6 and either GFP (closed circles) or FHF2B-GFP (open circles). For activation, cells were held at −120 mV and depolarized to a range of potentials (−65 to +20), and the normalized conductance was plotted as a function of voltage. For inactivation, cells were held at −120 mV, and the peak current amplitude was measured by a 40 msec test pulse to −10 mV, after 500 msec prepulses to potentials over the range −120 to +20 mV. Boltzmann fits to the data are shown. FHF2B caused a significant ($p < 0.02$) depolarizing shift in inactivation but no shift in activation parameters. *B*, Development of closed state inactivation at −70 mV was measured and showed greater inactivation with GFP transfected (closed circles) than FHF2B transfected cells (open circles). Lines are drawn to guide the eye. Cells were held at −120 mV, prepulsed to −70 mV for increasing amounts of time (1–3000 msec) and then stepped to −10 mV to determine the fraction of current inactivated during the prepulse. These data are consistent with the depolarizing shift in steady-state inactivation shown in *A*. *C*, Recovery from inactivation at −80 mV was measured and showed no differences between GFP-transfected (closed circles) and FHF2B-transfected (open circles) cells. Lines are drawn to guide the eye. Cells were held at −120 mV, and the peak current amplitude was measured by a test pulse to −10 mV, after a 40 msec inactivating pulse to −10 mV and a recovery period between 0.1 and 200 msec at −80 mV.

In situ hybridization for FHF2B in Purkinje cells, retinal ganglia cells, and ventral motor horn cell bodies

To further understand the basis for the absence of FHF2 labeling at the nodes of Ranvier in ventral root and optic nerve, we used *in situ* hybridization to investigate the expression of FHF2 mRNA in the motor neuron cell bodies in the ventral horn of the spinal cord, which project the fibers in the motor root, and in the retinal ganglion cells, which give rise to the fibers to the optic nerve. We also studied cerebellar Purkinje cells. All of the tissues were processed in parallel and, to compare levels of expression of FHF2 in these different tissues, the colorimetric reaction to detect the hybridized riboprobe was stopped when the signal was strong in any one tissue. *In situ* hybridization experiments show abundant expression of FHF2 in DRG neurons (Fig. 6*A*) compared with an absence of signal above background levels in cell bodies of motor neurons (Fig. 6*B*), cerebellar Purkinje neurons (Fig. 6*C*), and retinal ganglion cells (Fig. 6*D*). Thus, the lack of detectable FHF2 at the nodes of Ranvier along axons in the optic nerve and motor root is likely attributable to the low levels of FHF2 synthesis in the cell bodies that give rise to these axons.

FHF2B increases the amplitude of $Na_v1.6$ current in ND7/23 cells

To examine the functional consequences of coexpression of $Na_v1.6$ and FHF2B, we analyzed the sodium current density in the cell line ND7/23 transfected with GFP or with FHF2B-GFP. ND7/23 cells transiently transfected with GFP alone, $Na_v1.6_R$ and GFP, or $Na_v1.6_R$ and FHF2B-GFP were analyzed by whole-cell voltage-clamp electrophysiology (Fig. 7). Only cells with a robust green fluorescence signal were used for electrophysiological recording. All endogenous ND7/23 currents were blocked by the presence of TTX (6.0 ± 0.5 pA/pF; $n = 11$). ND7/23 cells transiently transfected with $Na_v1.6_R$ and GFP constructs produced a robust sodium current (Fig. 7*A*), unlike HEK 293 cells, which produce attenuated $Na_v1.6$ currents (data not shown). Coexpression of FHF2B-GFP and $Na_v1.6_R$ in ND7/23 cells produced a greater than twofold increase ($p < 0.001$) in the current density (Fig. 7*B*) compared with expression of $Na_v1.6_R$ and GFP. Figure 7*C* shows that cotransfection of $Na_v1.6_R$ and GFP produces a current density of 85.4 ± 21.2 pA/pF ($n = 11$), whereas cotransfection of $Na_v1.6_R$ and FHF2B-GFP increases the density substantially to 202.5 ± 17.2 pA/pF ($n = 22$; $p < 0.001$). Thus, in comparison with $Na_v1.6_R$ alone, the coexpression of FHF2B-GFP with $Na_v1.6_R$ causes a significant increase ($p < 0.001$) in current density. The expression of FHF2B-GFP in ND7/23 cells did not significantly change ($p > 0.05$) the capacitance of these cells (25.4 ± 1.9 pF; $n = 22$) compared with ND7/23 cells transfected with GFP (21.8 ± 1.1 pF; $n = 11$).

Table 1. Comparison of voltage-dependent properties of $Na_v1.6$ in ND7/23 cells coexpressing GFP or FHF2B-GFP

			Recovery from inactivation		
Condition	Activation $V_{1/2}$ (mV)	Inactivation $V_{1/2}$ (mV)	τ_1 at −80 mV (msec)	τ_2 at −80 mV (msec)	τ_1 Fraction
GFP	−18 ± 0.7 ($n = 11$)	−68 ± 1.4 ($n = 8$)	0.05 ± 0.01	11.9 ± 1.0	0.17 ± 0.05 ($n = 5$)
FHF2B-GFP	−19 ± 0.9 ($n = 22$)	−64 ± 0.4 ($n = 20$)*	0.07 ± 0.02	11.1 ± 0.3	0.18 ± 0.03 ($n = 14$)

Summary of fitted electrophysiological parameters for activation, inactivation (Boltzmann fits), and recovery from inactivation (double exponential fit). (See Materials and Methods for equations). There was a 4 mV depolarizing shift in channel inactivation properties with transfection of FHF2B, when compared with GFP. No other significant changes were found.

*$p < 0.02$ compared with GFP.

We also investigated the effects of FHF2B on the biophysical properties of the $Na_v1.6$ current. ND7/23 cells cotransfected with FHF2B-GFP and $Na_v1.6_R$ exhibited currents characterized by fast activation and inactivation, and fast recovery from inactivation (repriming) similar to the current that is recorded from DRG neurons that were transfected with the same construct (Herzog et al., 2003b). Figure 8 shows the normalized *I–V* relationship and steady-state inactivation (Fig. 8*A*), the rate of development of inactivation (Fig. 8*B*), and recovery from inactivation (Fig. 8*C*). Table 1 summarizes the electrophysiological properties of the $Na_v1.6_R$ current when coexpressed with GFP or FHF2B-GFP. These data demonstrate that there is no shift in the voltage dependence of activation but that there is a significant ($p < 0.02$) 4 mV depolarizing shift in the voltage dependence of steady-state inactivation. Consistent with the depolarizing shift in inactivation, plots of the development of inactivation of $Na_v1.6_R$ at −70 mV show significantly less inactivation of current when $Na_v1.6_R$ is coexpressed with FHF2B-GFP compared with coexpression with GFP (Fig. 8*B*). Finally, FHF2B does not change properties of recovery from inactivation when measured at −80 mV (Fig. 8*C*).

Discussion

We used a Y2H screen to identify protein partners of the TTX-S sodium channel $Na_v1.6$. We present evidence that FHF2, which is a member of the FGF family of growth factors (Smallwood et al., 1996), binds to the C-terminal polypeptide of $Na_v1.6$. We also present evidence that this interaction occurs *in vivo*. Importantly, we demonstrate that $Na_v1.6$ and FHF2 are colocalized at the nodes of Ranvier along dorsal root, but not ventral root, axons. This is the first demonstration of the differential distribution of a protein at the nodes of Ranvier of axons of distinct functional modality. Because the interaction between FHF2B and $Na_v1.6$ in a DRG-derived neuronal cell line significantly increases the amplitude of the $Na_v1.6$ current and causes a 4 mV shift in the voltage dependence of inactivation of the channel, our results suggest that the preferential expression of FHF2 in dorsal root axons may endow them with different physiological properties compared with ventral root axons.

The results of this study show that two FHF2 isoforms, which differ in their N terminus because of alternative splicing of exon 1 (Munoz-Sanjuan et al., 2000), can bind to $Na_v1.6$ in the Y2H assay. We have shown that a derivative of FHF2 that lacks the N terminus binds to the C terminus of $Na_v1.6$. Recently, the structure of FHF1B has been determined, and it has been shown that the core of the protein encoded by exons 2–4, which is ~70% identical to members of the FHF subfamily including FHF2 (Goldfarb, 2001), consists of a β-trefoil structure and that the integrity of this structure is required for the binding to the scaffold protein IB2 (Olsen et al., 2003). The inability of alternative isoforms of FHF2 to bind the $Na_v1.6$ C terminus in the Y2H assay suggests that the different N-terminal sequences may affect the binding of the two proteins either by steric hindrance or by reducing the affinity of the binding. The tolerance of the initial Y2H library screen in the Matchmaker system, which identified FHF4 as another binding partner to the $Na_v1.6$ C terminus, for weaker interactions might be higher than that of the Proquest Y2H system that was used for the analysis shown in Figure 1. Thus, it is possible that all FHF2 isoforms, as well as the FHF4 isoforms, can be partners of $Na_v1.6$ *in vivo*.

The C termini of multiple sodium channels have been implicated in the regulation of their inactivation properties (Deschenes et al., 2001; Mantegazza et al., 2001; Cormier et al., 2002). Previously, we have shown that the membrane-proximal stretch of the C terminus of $Na_v1.5$ and $Na_v1.9$, which we have called conserved region 1 (CR1) because it is ~70% identical among the sodium channels, is important for the interaction of these channels with FHF1B (Liu et al., 2001, 2003) and that the interaction of FHF1B and $Na_v1.5$ causes a hyperpolarizing shift in the voltage dependence of channel inactivation (Liu et al., 2003). The analogous CR1 sequence of $Na_v1.6$ is also critical for the binding of FHF2B (data not shown). However, we show in this study that the interaction of FHF2B with $Na_v1.6$ causes a depolarizing shift in the voltage dependence of inactivation, together with a significant increase in the peak current amplitude. Therefore, it appears that the interactions of different channels and members of the FHF family produce distinct changes in current amplitude and kinetics.

The mechanism(s) underlying the robust increase in current amplitude of recombinant $Na_v1.6$, which is associated with coexpression of FHF2B, has yet to be determined. FHF2B may induce the insertion of more channels from a cytosolic pool into the membrane. An alternative is the recruitment of a kinase to the channel complex and the subsequent phosphorylation of the channel. Phosphorylation of sodium channels by PKA and PKC has been shown to either increase or decrease the peak current amplitude, depending on the channel isoform (Fitzgerald et al., 1999; Cantrell and Catterall, 2001; Vijayaragavan et al., 2004). Another alternative is that the binding of FHF2B to the C terminus may increase the probability of channel opening upon depolarization. Additional studies are underway to determine the relative contribution of these alternative mechanisms to the FHF2B-induced upregulation of the $Na_v1.6$ current.

$Na_v1.6$ is the major sodium channel at mature nodes of Ranvier in myelinated fibers in both the PNS and CNS (Caldwell et al., 2000; Krzemien et al., 2000; Tzoumaka et al., 2000; Boiko et al., 2001). The rapidly activating and inactivating $Na_v1.6$ current is characterized by fast recovery from inactivation (Herzog et al., 2003b). This appears to poise $Na_v1.6$ for high-frequency firing of myelinated fibers that do not, however, fire in response to sustained slow depolarizations (Kocsis et al., 1983). The selective presence of FHF2 at the nodes of Ranvier in peripheral sensory fibers, together with our observation that its association with $Na_v1.6$ increases the current amplitude significantly, suggests that the association of $Na_v1.6$ and FHF2 at the nodes of Ranvier can be functionally relevant and may influence the electrogenic properties of nodes along these sensory axons. Indeed, there is

electrophysiological data to suggest a distinction in the electrogenic properties of motor and sensory fibers of the PNS. As early as 1938, it was reported that sensory axons, unlike motor axons, are more likely to fire repeatedly in response to a maintained stimulus (Erlanger and Blair, 1938). Sensory fibers have been shown to have a greater propensity to fire ectopically on release from ischemia (Bostock et al., 1994). In addition, immature (Bowe et al., 1985) and demyelinated (Bowe et al., 1987) dorsal root axons display burst activity that is not seen in ventral root axons after potassium channel blockade with 4-AP. Moreover, sensory and motor fibers are both susceptible to different injuries, with motor fibers being selectively affected in some neuropathies and sensory fibers preferentially affected in others. Although the selective expression of $Na_v1.8$ in DRG neurons (Akopian et al., 1996; Djouhri et al., 2003) reduces accommodation (Renganathan et al., 2001) and may thus contribute to the physiological properties of sensory axons, there are other factors, in addition to the selective expression of various sodium channel subtypes, that shape the functional characteristics of sensory nerve fibers. We suggest that the differential expression of FHF2 and its association with $Na_v1.6$ at the nodes of Ranvier in dorsal root fibers contributes to the differences between the biophysical properties of sensory and motor fibers.

References

Akopian AN, Sivilotti L, Wood JN (1996) A tetrodotoxin-resistant voltage-gated sodium channel expressed by sensory neurons. Nature 379:257–262.

Black JA, Dib-Hajj S, McNabola K, Jeste S, Rizzo MA, Kocsis JD, Waxman SG (1996) Spinal sensory neurons express multiple sodium channel alpha-subunit mRNAs. Mol Brain Res 43:117–131.

Black JA, Renganathan M, Waxman SG (2002) Sodium channel Na(v)1.6 is expressed along nonmyelinated axons and it contributes to conduction. Mol Brain Res 105:19–28.

Boiko T, Rasband MN, Levinson SR, Caldwell JH, Mandel G, Trimmer JS, Matthews G (2001) Compact myelin dictates the differential targeting of two sodium channel isoforms in the same axon. Neuron 30:91–104.

Bostock H, Burke D, Hales JP (1994) Differences in behaviour of sensory and motor axons following release of ischaemia. Brain 117:225–234.

Bowe CM, Kocsis JD, Waxman SG (1985) Differences between mammalian ventral and dorsal spinal roots in response to blockade of potassium channels during maturation. Proc R Soc Lond B Biol Sci 224:355–366.

Bowe CM, Kocsis JD, Targ EF, Waxman SG (1987) Physiological effects of 4-aminopyridine on demyelinated mammalian motor and sensory fibers. Ann Neurol 22:264–268.

Burgess DL, Kohrman DC, Galt J, Plummer NW, Jones JM, Spear B, Meisler MH (1995) Mutation of a new sodium channel gene, Scn8a, in the mouse mutant "motor endplate disease." Nat Genet 10:461–465.

Caldwell JH, Schaller KL, Lasher RS, Peles E, Levinson SR (2000) Sodium channel Na(v)1.6 is localized at nodes of Ranvier, dendrites, and synapses. Proc Natl Acad Sci USA 97:5616–5620.

Cantrell AR, Catterall WA (2001) Neuromodulation of Na+ channels: an unexpected form of cellular plasticity. Nat Rev Neurosci 2:397–407.

Catterall WA (2000) From ionic currents to molecular mechanisms: the structure and function of voltage-gated sodium channels. Neuron 26:13–25.

Cormier JW, Rivolta I, Tateyama M, Yang AS, Kass RS (2002) Secondary structure of the human cardiac Na+ channel carboxy terminus: Evidence for a role of helical structures in modulation of channel inactivation. J Biol Chem 277:9233–9241.

Deschenes I, Trottier E, Chahine M (2001) Implication of the C-terminal region of the alpha-subunit of voltage-gated sodium channels in fast inactivation. J Membr Biol 183:103–114.

Deschenes I, Neyroud N, DiSilvestre D, Marban E, Yue DT, Tomaselli GF (2002) Isoform-specific modulation of voltage-gated Na(+) channels by calmodulin. Circ Res 90:E49–E57.

Dib-Hajj SD, Tyrrell L, Black JA, Waxman SG (1998) NaN, a novel voltage-gated Na channel, is expressed preferentially in peripheral sensory neurons and down-regulated after axotomy. Proc Natl Acad Sci USA 95:8963–8968.

Dietrich PS, McGivern JG, Delgado SG, Koch BD, Eglen RM, Hunter JC, Sangameswaran L (1998) Functional analysis of a voltage-gated sodium channel and its splice variant from rat dorsal root ganglia. J Neurochem 70:2262–2272.

Djouhri L, Fang X, Okuse K, Wood JN, Berry CM, Lawson S (2003) The TTX-resistant sodium channel Nav1.8 (SNS/PN3): expression and correlation with membrane properties in rat nociceptive primary afferent neurons. J Physiol (Lond) 550:739–752.

Erlanger J, Blair E (1938) Comparative observations on motor and sensory fibers with special reference to repetitiosness. Am J Physiol 121:431–453.

Fang X, Djouhri L, Black JA, Dib-Hajj SD, Waxman SG, Lawson SN (2002) The presence and role of the tetrodotoxin-resistant sodium channel Na(v)1.9 (NaN) in nociceptive primary afferent neurons. J Neurosci 22:7425–7433.

Fitzgerald EM, Okuse K, Wood JN, Dolphin AC, Moss SJ (1999) cAMP-dependent phosphorylation of the tetrodotoxin-resistant voltage- dependent sodium channel SNS. J Physiol (Lond) 516:433–446.

Goldfarb M (2001) Signaling by fibroblast growth factors: the inside story. Sci STKE 2001:PE37.

Goldin AL, Barchi RL, Caldwell JH, Hofmann F, Howe JR, Hunter JC, Kallen RG, Mandel G, Meisler MH, Netter YB, Noda M, Tamkun MM, Waxman SG, Wood JN, Catterall WA (2000) Nomenclature of voltage-gated sodium channels. Neuron 28:365–368.

Herzog RI, Liu C, Waxman SG, Cummins TR (2003a) Calmodulin binds to the C terminus of sodium channels Nav1.4 and Nav1.6 and differentially modulates their functional properties. J Neurosci 23:8261–8270.

Herzog RI, Cummins TR, Ghassemi F, Dib-Hajj SD, Waxman SG (2003b) Distinct repriming and closed-state inactivation kinetics of Nav1.6 and Nav1.7 sodium channels in mouse spinal sensory neurons. J Physiol (Lond) 551:741–750.

Hollenberg SM, Sternglanz R, Cheng PF, Weintraub H (1995) Identification of a new family of tissue-specific basic helix-loop- helix proteins with a two-hybrid system. Mol Cell Biol 15:3813–3822.

Jenkins SM, Bennett V (2001) Ankyrin-G coordinates assembly of the spectrin-based membrane skeleton, voltage-gated sodium channels, and L1 CAMs at Purkinje neuron initial segments. J Cell Biol 155:739–746.

John VH, Main MJ, Powell AJ, Gladwell ZM, Hick C, Sidhu HS, Clare JJ, Tate S, Trezise DJ (2004) Heterologous expression and functional analysis of rat Na(V)1.8 (SNS) voltage-gated sodium channels in the dorsal root ganglion neuroblastoma cell line ND7–23. Neuropharmacology 46:425–438.

Kocsis JD, Ruiz JA, Waxman SG (1983) Maturation of mammalian myelinated fibers: Changes in action-potential characteristics following 4-aminopyridine application. J Neurophysiol 50:449–463.

Krzemien DM, Schaller KL, Levinson SR, Caldwell JH (2000) Immunolocalization of sodium channel isoform NaCh6 in the nervous system. J Comp Neurol 420:70–83.

Li GD, Wo Y, Zhong MF, Zhang FX, Bao L, Lu YJ, Huang YD, Xiao HS, Zhang X (2002) Expression of fibroblast growth factors in rat dorsal root ganglion neurons and regulation after peripheral nerve injury. NeuroReport 13:1903–1907.

Liu C, Dib-Hajj SD, Waxman SG (2001) Fibroblast growth factor homologous factor 1B binds to the C terminus of the tetrodotoxin-resistant sodium channel rNav1.9a (NaN). J Biol Chem 276:18925–18933.

Liu C, Dib-Hajj SD, Renganathan M, Cummins TR, Waxman SG (2003) Modulation of the cardiac sodium channel Nav1.5 by fibroblast growth factor homologous factor 1B. J Biol Chem 278:1029–1036.

Mantegazza M, Yu FH, Catterall WA, Scheuer T (2001) Role of the C-terminal domain in inactivation of brain and cardiac sodium channels. Proc Natl Acad Sci USA 98:15348–15353.

Meisler MH, Kearney JA, Sprunger LK, MacDonald BT, Buchner DA, Escayg A (2002) Mutations of voltage-gated sodium channels in movement disorders and epilepsy. Novartis Found Symp 241:72–81.

Mori M, Konno T, Ozawa T, Murata M, Imoto K, Nagayama K (2000) Novel interaction of the voltage-dependent sodium channel (VDSC) with calmodulin: does VDSC acquire calmodulin-mediated Ca2+-sensitivity? Biochemistry 39:1316–1323.

Munoz-Sanjuan I, Smallwood PM, Nathans J (2000) Isoform diversity among fibroblast growth factor homologous factors is generated by alternative promoter usage and differential splicing. J Biol Chem 275:2589–2597.

Olsen SK, Garbi M, Zampieri N, Eliseenkova AV, Ornitz DM, Goldfarb M,

Mohammadi M (2003) Fibroblast growth factor (FGF) homologous factors share structural but not functional homology with FGFs. J Biol Chem 278:34226–34236.

Peles E, Salzer JL (2000) Molecular domains of myelinated axons. Curr Opin Neurobiol 10:558–565.

Ratcliffe CF, Westenbroek RE, Curtis R, Catterall WA (2001) Sodium channel beta1 and beta3 subunits associate with neurofascin through their extracellular immunoglobulin-like domain. J Cell Biol 154:427–434.

Renganathan M, Cummins TR, Waxman SG (2001) Contribution of Na(v)1.8 sodium channels to action potential electrogenesis in DRG neurons. J Neurophysiol 86:629–640.

Schaller KL, Krzemien DM, Yarowsky PJ, Krueger BK, Caldwell JH (1995) A novel, abundant sodium channel expressed in neurons and glia. J Neurosci 15:3231–3242.

Schoorlemmer J, Goldfarb M (2002) Fibroblast growth factor homologous factors and the islet brain-2 scaffold protein regulate activation of a stress-activated protein kinase. J Biol Chem 277:49111–49119.

Smallwood PM, Munoz-Sanjuan I, Tong P, Macke JP, Hendry SH, Gilbert DJ, Copeland NG, Jenkins NA, Nathans J (1996) Fibroblast growth factor (FGF) homologous factors: new members of the FGF family implicated in nervous system development. Proc Natl Acad Sci USA 93:9850–9857.

Smith MR, Smith RD, Plummer NW, Meisler MH, Goldin AL (1998) Functional analysis of the mouse Scn8a sodium channel. J Neurosci 18:6093–6102.

Tan HL, Kupershmidt S, Zhang R, Stepanovic S, Roden DM, Wilde AA, Anderson ME, Balser JR (2002) A calcium sensor in the sodium channel modulates cardiac excitability. Nature 415:442–447.

Tzoumaka E, Tischler AC, Sangameswaran L, Eglen RM, Hunter JC, Novakovic SD (2000) Differential distribution of the tetrodotoxin-sensitive rPN4/NaCh6/Scn8a sodium channel in the nervous system. J Neurosci Res 60:37–44.

Vijayaragavan K, Boutjdir M, Chahine M (2004) Modulation of Nav1.7 and Nav1.8 peripheral nerve sodium channels by protein kinase A and protein kinase C. J Neurophysiol 91:1556–1569.

Wood JN, Bevan SJ, Coote PR, Dunn PM, Harmar A, Hogan P, Latchman DS, Morrison C, Rougon G, Theveniau M (1990) Novel cell lines display properties of nociceptive sensory neurons. Proc R Soc Lond B Biol Sci 241:187–194.

Zhou X, Dong XW, Crona J, Maguire M, Priestley T (2003) Vinpocetine is a potent blocker of rat NaV1.8 TTX-resistant sodium channels. J Pharmacol Exp Ther 306:498–504.